

IN SILICO CHARACTERIZATION, MOLECULAR DOCKING, AND IN VITRO EVALUATION OF TRIAZOLE DERIVATIVES AS POTENTIAL ANTICANCER AGENTS

HARSHITHA T, VINAY KUMAR T*, VINEETHA T

Department of Pharmacology, Nirmala College of Pharmacy, Atmakur, Andhra Pradesh, India. Email: vinaykumartheendra@gmail.com

Received: 24 October 2020, Revised and Accepted: 30 November 2020

ABSTRACT

Objective: The objective of the study was to perform *in silico* molecular docking and *in vitro* anticancer studies of proposed 1,2,4-triazole derivatives for the determination of their anticancer activity.

Methods: A series of 10 triazole compounds with different substituents were drawn in ACD Lab ChemSketch software. Molecular and biological properties were identified using Molinspiration software. The compounds that obeyed Lipinski rule of five are subjected for pharmacokinetic parameters prediction and docking analysis. SwissDock ADME software is used for the prediction of absorption, distribution, metabolism, and elimination. Then, the compounds are docked with target enzymes in Chimera software 1.14 version. The molecular docking studies revealed favorable molecular interactions and binding energies. The compounds that showed good docking results were synthesized through wet lab synthesis and further preceded for *in vitro* anticancer studies.

Results: Three compounds are selected for wet lab synthesis due to their good docking results compared to other compounds. The synthesized compounds are subjected to different *in vitro* anticancer studies and found to be having potential anticancer activity.

Conclusion: The pharmacokinetic and docking studies conclude that the triazole compounds have potential as anticancer agents. The *in vitro* anticancer studies revealed that the triazole derivatives are having high potency of anticancer activity against pancreatic cell lines.

Keywords: Molinspiration, SwissDock, ADME and Chimera, Neutral red reuptake assay, Cell lines, etc.

© 2021 The Authors. Published by Innovare Academic Sciences Pvt Ltd. This is an open access article under the CC BY license (<http://creativecommons.org/licenses/by/4.0/>) DOI: <http://dx.doi.org/10.22159/ajpcr.2021v14i2.40053>. Journal homepage: <https://innovareacademics.in/journals/index.php/ajpcr>

INTRODUCTION

Mitogen-activated pathway (MAP kinase) involves a series of proteins that interface a signal from receptor that is present on the surface of the cell to the DNA present in the nucleus, which regulates the gene expression, cellular growth and apoptosis, etc. [7]. Any alterations in the MAP kinase pathway lead to tumorigenicity of cells and resistance to apoptosis [8]. Protein kinases are the enzymes that catalyze protein phosphorylation through adenosine triphosphate and convert inactive protein into active protein regulating the biological activity of protein. Deregulated kinases are found to be central for survival and spread of cancer cells. Tyrosine kinase is the subclass of protein kinases [9,10].

Heat shock proteins play an important role in protein interactions such as folding and assisting in the protein conformation and prevention of protein aggregation. These are released during stress conditions. Their distinctive interaction with the oncogenes excels the progression of individual cancer [11,12]. The (3-(4,5-dimethylthiazol-2-yl)-2,5-diphenyltetrazolium bromide) (MTT) assay is a colorimetric assay for measuring cell metabolic activity. It is based on the ability of nicotinamide adenine dinucleotide phosphate-dependent cellular oxidoreductase enzymes to reduce the tetrazolium dye MTT to its insoluble formazan, which has a purple color [18]. In the MTT assay, a solubilization solution (dimethyl sulfoxide or acidified ethanol solution or a solution of the detergent sodium dodecyl sulfate in diluted hydrochloric acid) is added to dissolve the insoluble purple formazan product into a colored solution. The absorbance of this colored solution can be quantified by measuring at a certain wavelength (usually between 500 and 600 nm) by a spectrophotometer. MTT method is one of the most widely used methods to analyze cell proliferation and viability [20]. The neutral red (NR) uptake assay provides a quantitative estimation of the number of viable cells in a culture. It is based on the ability of viable cells to incorporate and bind the supravital dye NR in the

lysosomes. Most primary cells and cell lines from diverse origin may be successfully used. Cells are seeded in 96-well tissue culture plates and are treated for the appropriate period. The plates are then incubated for 2 h with a medium containing NR. The cells are subsequently washed, the dye is extracted in each well, and the absorbance is read using a spectrophotometer.

METHODS

Preparation of triazole structure

Ten number of triazole derivatives were prepared *in-silico* molecular modifications at R1 and R2 positions using ACD Lab ChemSketch software, Fig. 1. Three-dimensional (3D) drawing, optimizing, and calculating various molecular descriptors of proposed derivatives were done using ACD Lab ChemSketch software, Table 1.

Calculation of biological properties

The Molinspiration software was used to study the LogP values, violation of Lipinski's rule of five and druglikeness, etc. [21,22]. The smiles are used to calculate the biological properties. The results are shown in Tables 2 and 3.

Prediction of absorption, distribution, metabolism, and elimination (ADME) properties

SwissDock ADME software is used for the prediction of pharmacodynamic properties such as ADME. The prediction of ADME properties helps to eliminate the less potential drugs before the start of synthesis and trials of drug [23]. The results are shown in Table 4.

Glide score

The glide score of the selected five compounds is obtained through Schrodinger trial version software. The results are displayed in Table 5.

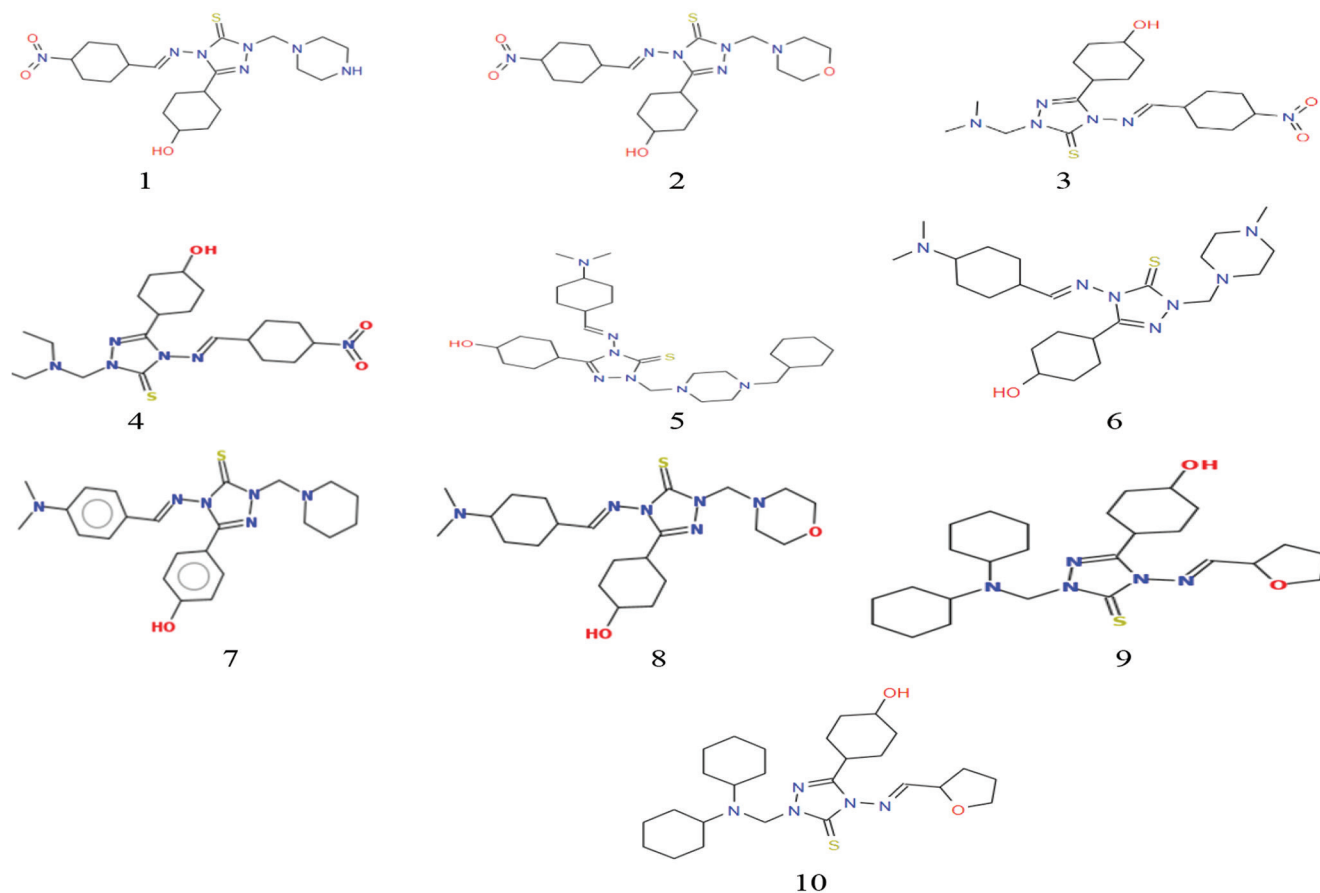


Fig. 1: Chemical structures of proposed triazole derivatives

Table 1: Molecular descriptors of proposed 1,2,4-triazole derivatives

S. No.	Molecular formula	Molar refractivity Cm ³ (±0.5)	Molecular weight	Surface tension Dyne/cm (±7.0)	Polarisibility 10 ⁻²⁴ cm ³ (±0.5)
1.	C ₂₀ H ₂₁ N ₇ O ₃ S	119.39	439.49	65.75	47.33
2.	C ₂₀ H ₂₀ N ₆ O ₄ S	117.72	440.47	64.01	46.68
3.	C ₁₈ H ₁₈ N ₆ O ₃ S	109.29	398.88	57.32	43.32
4.	C ₂₀ H ₂₂ N ₆ O ₃ S	118.51	426.49	54.72	46.98
5.	C ₂₆ H ₃₃ N ₇ O ₃ S	157.15	527.68	50.04	62.30
6.	C ₂₃ H ₂₉ N ₇ O ₃ S	131.23	451.35	50.15	52.37
7.	C ₂₂ H ₂₈ N ₆ O ₃ S	128.09	436.57	50.06	50.77
8.	C ₂₂ H ₂₆ N ₆ O ₃ S	124.87	438.54	51.35	49.50
9.	C ₁₈ H ₂₁ N ₅ O ₂ S	105.02	371.45	41.63	41.63
10.	C ₁₉ H ₂₁ N ₅ O ₂ S	107.47	383.46	56.62	42.59

Docking studies

The docking studies were done using Molecule docking software. This software has been developed by Robert Kriss, Mark Sandor, Zoltanzalai, Ferenc Szalai, and Lazlo Havancsak. It offers database and modeling tools.

Protein/target preparation

Nearly 10,000 automatically prepared target structures integrated from the PDB database. All the Protein structures are represented in PDB format, which is used for Docking studies. We can also draw the structures as drawing tool is available or we can upload the files in pdb/mol². The target molecules are selected from the database and their 3D structure appears.

Ligand preparation

If the ligand molecule is available in software database, then we can select that structure. If the ligand molecule is new molecule, then we can draw our structure or we can upload the file in mol². format. This software

uses the Autodock Vina algorithm, the Autodock tools are utilized automatically for structure editing such as addition of hydrogen charges if none exists, adds Gasteiger charges, merges charges, and removes lone pairs non-polar hydrogen, non-standard residues water molecules.

Docking

The docking was performed through Autodock Vina and results were displayed after docking. The results are shown in Table 6.

Wet lab synthesis

The samples that showed good docking scores are further synthesized through wet lab synthesis and analyzed through IR spectra for their molecular groups.

Characterization of compounds by infrared (IR) spectral study

The Fourier transform IR (FTIR) is used for the identification of organic and inorganic molecular components and structure. FTIR spectroscopy

Table 2: Lipinski's rule analysis of proposed 1,2,4-triazole derivatives

S. No.	Molecular formula	Mi Log P	Mol. Wt	HAC	HBDO	Rot bonds	Violation
1.	C ₂₀ H ₂₁ N ₇ O ₃ S	0.13	451.60	10	2	6	0
2.	C ₂₀ H ₂₀ N ₆ O ₄ S*	2.41	44.49	10	1	6	0
3.	C ₁₈ H ₁₈ N ₆ O ₃ S	0.83	410.54	9	1	6	1
4.	C ₂₀ H ₂₂ N ₆ O ₃ S*	1.58	438.60	9	1	8	0
5.	C ₂₉ H ₃₃ N ₇ OS	3.26	545.84	8	1	6	1
6.	C ₂₃ H ₂₉ N ₇ OS	0.92	463.70	8	1	6	1
7.	C ₂₃ H ₂₈ N ₆ OS*	3.61	436.58	7	1	6	0
8.	C ₂₂ H ₂₆ N ₅ OS*	0.92	450.65	8	1	6	0
9.	C ₁₈ H ₂₁ N ₅ O ₂ S*	3.93	489.73	7	1	7	0
10.	C ₁₉ H ₂₁ N ₅ O ₂ S	1.03	393.56	7	1	5	1

M.W: Molecular weight, HAC: Number of hydrogen bond acceptor, HDO: Number of hydrogen bond donor, rot b: Number of rotatable bonds

Table 3: Molinspiration bioactivity score

S. No.	Molecular formula	GPCR ligand (-)	Ion channel modulator (-)	Kinase inhibitor (-)	Nuclear receptor ligand (-)	Protease inhibitor (-)	Enzyme inhibitor (-)
1.	C ₂₀ H ₂₁ N ₇ O ₃ S	0.55	0.56	0.75	0.93	0.61	0.37
2.	C ₂₀ H ₂₀ N ₆ O ₄ S*	0.85	0.87	0.82	0.90	0.89	0.65
3.	C ₁₈ H ₁₈ N ₆ O ₃ S	0.67	0.61	0.88	0.93	0.69	0.45
4.	C ₂₀ H ₂₂ N ₆ O ₃ S*	0.64	0.65	0.85	0.93	0.72	0.42
5.	C ₂₉ H ₃₃ N ₇ OS	0.27	0.54	0.52	0.78	0.41	0.28
6.	C ₂₃ H ₂₉ N ₇ OS	0.37	0.53	0.88	0.90	0.52	0.31
7.	C ₂₃ H ₂₈ N ₆ OS*	0.81	0.95	0.85	1.02	1.06	0.60
8.	C ₂₂ H ₂₆ N ₅ OS*	0.43	0.62	0.61	0.92	0.53	0.54
9.	C ₁₈ H ₂₁ N ₅ O ₂ S*	0.46	0.57	0.64	0.73	0.48	0.37
10.	C ₁₉ H ₂₁ N ₅ O ₂ S	0.64	0.81	0.84	0.99	0.73	0.51

The compounds with star mark have shown better properties and obeyed the Lipinski rule of five than the remaining compounds. Hence, these five compounds were docked in Chimera software and analyzed for their ADME properties

Table 4: ADME prediction scores

Molecular formula	Lipophilicity (log P _{ow})	Water solubility (Log S)	GI absorption	CYP _{3A4} inhibitor	Synthetic accessibility
C ₂₀ H ₂₀ N ₆ O ₄ S (sample 1)	-2.26	Soluble	Low	No	5.77
C ₂₀ H ₂₂ N ₆ O ₃ S (sample 2)	-2.00	Moderately soluble	Low	Yes	5.93
C ₂₃ H ₂₈ N ₆ OS (sample 3)	-4.72	Soluble	High	Yes	5.84
C ₂₂ H ₂₆ N ₅ OS (sample 4)	-4.45	Soluble	High	Yes	5.75
C ₁₈ H ₂₁ N ₅ O ₂ S (sample 5)	-4.06	Moderately soluble	High	No	5.02

Table 5: Glide scores of the compounds

S. No.	Compounds	Glide score
1.	Sample 1	-7.63
2.	Sample 2	-7.19
3.	Sample 3	-8.28
4.	Sample 4	-9.68
5.	Sample 5	-7.52

is an analytical technique used to identify organic (and in some cases inorganic) materials. This technique measures the absorption of IR radiation by the sample material versus wavelength.

All the IR spectra are measured using a FTIR-4100 type. The spectral resolution of the instrument is 0.25 cm⁻¹, and the spectral data are stored in the database at the intervals of 0.5 cm⁻¹ at 4000-2000 cm⁻¹ and of 0.25 cm⁻¹ at 2000-400 cm⁻¹.

Assessment of *in vitro* anticancer activity

Cell proliferation – MTT assay

The metabolic activity of growing cells was assessed by means of the MTT assay. In the test, yellow tetrazolium salt MTT is metabolized by viable cells to purple formazan crystals. HT-29 and A549 cells were plated on flat-bottom 96-well microplates at a density of 3×10⁴ cells/ml (HT-29) and 1×10⁴ (A549) cells/ml in 100 μl of a complete growth medium.

The next day, the culture medium was removed and the cells exposed to serial dilutions of HWE and HJE at concentrations ranging from 0.1 to 5 mg/ml. After 96 h incubation, the cells were incubated for 3 h with an MTT solution (5 mg/ml), and formazan crystals then solubilized overnight by adding SDS buffer (10% SDS in 0.01 N HCl).

The color product of the reaction was quantified by measuring absorbance at a 570 nm wavelength using an Emax Microplate Reader (Menlo Park, CA, USA). IC₅₀ was calculated using the computerized linear regression analysis of quantal log dose-probit functions, according to the method of Litchfield and Wilcoxon. Cell viability (%) was expressed as a percentage relative to the untreated control cells.

Cell viability – NR assay

The NR assay determines the accumulation of NR dye in the lysosomes of viable, uninjured cells. The HT-29, CCD 841 CoTr, A549, and human skin fibroblasts cells were plated on 96-well microplates at a density of 1×10⁵ cells/ml in a complete growth medium. After 24 h incubation, the growth medium was replaced by a fresh medium (containing 2% fetal bovine serum) and the cells exposed to serial dilutions of HWE and HJE (0.1–5 mg/ml). After 24 h, the cells were incubated with the NR reagent for 3 h, fixed with the NR fixative solution (1% CaCl₂ in 0.5% formalin) for 3 min at room temperature, and solubilized in 1% acetic acid in 50% ethanol under shaking for 20 min. Absorbance was measured at 550 nm using an E_{max} Microplate Reader.

Calculation of IC_{50} values

According to the Food and Drug Administration, IC_{50} represents the concentration of a drug that is required for 50% inhibition *in vitro*. EC_{50} also represents the plasma concentration required for obtaining 50% of a maximum effect *in vivo*. It is comparable to an EC_{50} for agonist drugs. The values were calculated using GraphPad Prism.

$$IC_{50} = \frac{(\text{Top} + \text{Baseline}) / 2 - \text{Bottom} + (\text{Top} - \text{Bottom}) / (1 + 10^{[(\text{Log}IC_{50} \times) * \text{HillSlope} + \log(\text{Top} - \text{Bottom}) / (\text{Fifty} - \text{Bottom})]} - 1)}$$

Note the distinction between the parameter bottom and baseline. Bottom is the Y value of the bottom plateau of the curve itself. Baseline is the Y value that defines 0% maximal inhibition by a standard drug. You'll definitely want to constrain baseline to be a constant value based on controls. You may also want to constrain top.

RESULTS AND DISCUSSION

Molinspiration

Molinspiration software is used to calculate the biological properties and to analyze the Lipinski rule of five. The results are shown in Tables 2 and 3.

Prediction of ADME properties

The selected compounds were analyzed for their ADME properties through SwissDock ADME software.

Glide score

The glide score results are shown below.

Docking results

The docking analysis is performed through Chimera software 1.14 version and the results are shown in Table 6 and the figures are shown in Fig. 2.

Evaluation of *in vitro* anticancer activity

In vitro Anticancer studies were done by MTT assay-% viability of PANC-1 (pancreatic cancer cell line) & Neutral red uptake assay.

DISCUSSION

Using ACD Lab ChemSketch, we have drawn 10 triazole derivatives and their molecular properties such as molar refractivity, surface tension, polarisability, and molecular weight. These all properties play an important role in the pharmacotherapy of the drug. Molecular weight is the total mass of the molecule or the sum of all the atoms present in the molecule. The molecular weight of any drug/biologics should be within the limits of below 1000 Daltons as it affects the absorption and distribution of drug. Smaller the size of the molecule, the absorption is fast and it can freely travel to any destination in the body without causing any obstructions. Furthermore, if the molecular weight is high means the size will also be increased and it causes the disturbance in ADME properties and also during manufacturing process [Tables 7

Table 6: Docking results: Binding energy of samples with target enzymes

Target enzyme	Sample 1 (-)	Sample 2 (-)	Sample 3 (-)	Sample 4 (-)	Sample 5 (-)
Protein kinase C	8.0	7.9	7.5	7.3	7.8
Tyrosine kinase	7.9	7.8	7.2	7.9	7.4
HSP90	7.4	7.4	7.4	7.2	8.2
Tubulin	8.0	6.3	7.9	7.3	7.4
MAP kinase	7.5	7.8	7.5	7.2	8.0

Based on the docking results, the samples 2,3,4 were subjected to wet lab synthesis and further proceeded to molecular characterization and *in vitro* anticancer studies

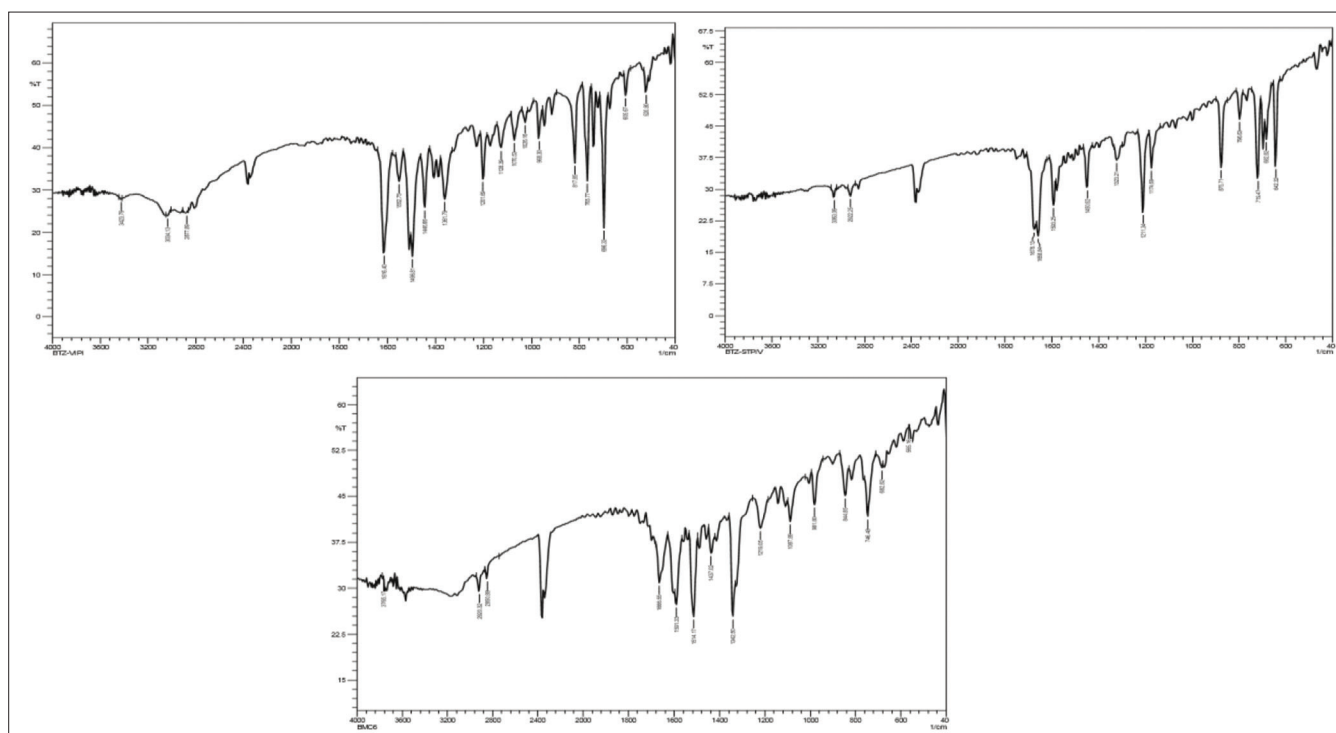


Fig. 2: Fourier transform infrared spectral images of samples 2, 3, and 4, respectively

and 8]. Hence, as shown in Table 1, all the compounds are in and around 400–500 range which is below 1000 Daltons. Molar refractivity is the

Table 7: FTIR studies for the synthesized compounds

S. No.	Compound	IR spectra
1.	Sample 2	O-H str (3423), C-H str of CH ₃ in DEA (3034), C-H str of Mannich base (2877, 2840), C=N str of triazole (1616), N=O str (1552), C=S (1201) (Fig. 2)
2.	Sample 3	O-H str (3634), C-H str of Mannich base (2922, 2827), C=N str of triazole (1678), C=S (1174), C-H str DMAB (3063) (Fig. 2)
3.	Sample 4	O-H str (3765), C-H str of Mannich base (2920, 2850), C=N str of triazole (1666), C-O-C str (1087), C=S str(1219), C-H str DMAB (3068) (Fig. 2)

Table 8: IC50 values of selected compounds on PANC⁻¹ (µg/mL)

S. No.	DRUG	IC50 value
1.	Paclitaxel (standard)	547.55±33.52
2.	Triazole derivative – A (sample 2)	557.66±50.24
3.	Triazole derivative – B (sample 3)	631.99±50.24
4.	Triazole derivative – C (sample 4)	523.88±50.24

Table 9: MTT assay-% viability of PANC-1 (pancreatic cancer cell line)

S. No.	Drug	% viability							
		Concentration (µg/ml)	3.1	6.3	12.5	25.0	50.0	100.0	200.0
1.	Negative control		96	96	96	96	96	96	96
2.	Paclitaxel (standard)		83	81	77	67	57	52	47
3.	Triazole derivative – A (sample 2)		69	63	65	62	60	54	46
4.	Triazole derivative – B (sample 3)		75	73	71	61	54	50	43
5.	Triazole derivative – C (sample 4)		72	68	66	60	58	53	47

From the results of MTT assay and IC50 values, the triazole derivative – B compound (sample 3) has shown the highest results. Hence, the sample 3 is further preceded for the cell line testing through neutral red uptake assay method. The results are shown in Fig. 2

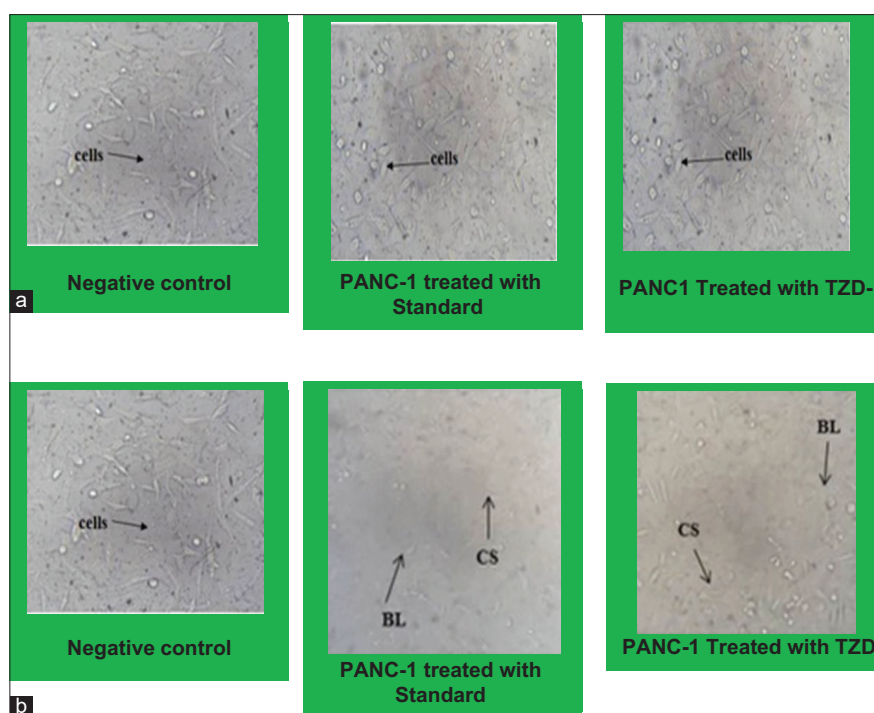


Fig. 3: Morphological changes in PANC-1 (pancreatic cancer cell line), (a): Before treatment with triazole derivative sample, (b): After treatment with triazole derivative sample

total polarisability of the molecule and is dependent on temperature, pressure, and the index of refraction. It is the real volume of molecule. It plays a role in the London forces that act in the drug receptor interaction. The molar refractive values are also within the range of 40–200, Table 1, etc.

Surface tension is the force exerted by the molecules that are present underneath on the surface layer which results in the shrinking of surface into the bulk of the compound. This results in the decreased surface area. There is a range of surface tension values for every dosage form and for oral, it is 36.6–65.7 dyne/cm and all the triazole derivatives are within the range. It mainly affects the solubility of the drug. Hence, as shown in Table 1, all these molecular properties are within the range of standards and so these triazole derivatives can be developed into dosage forms.

The Lipinski rule and its violation are verified in Molinspiration software as mentioned in Table 2. Lipinski rule states that there should not be more than 10 hydrogen acceptors and 5 hydrogen bond donors. All the compounds that violated the rule are eliminated from the further proceedings as they are unfit for docking process. The Lipinski rule plays major role in pharmacokinetics (ADME) rather than in pharmacodynamics of the drug. The biological activity such as enzyme inhibition and G protein-coupled receptors (GPCR) ligand inhibition was also calculated in this software, as shown in Table 3. GPCR ligand is the surface binding receptor that is involved in the signaling pathways of various diseases. Hence, GPCR inhibition is very important for the

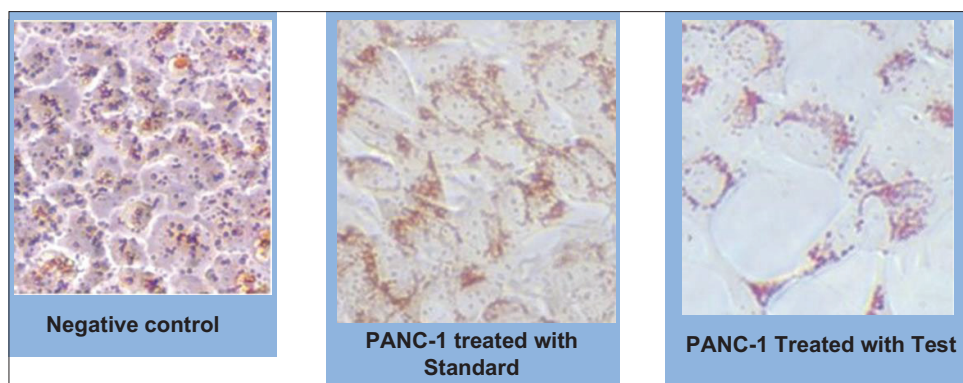


Fig. 4: Neutral red uptake test for cell viability changes in PANC-1

drug molecule. Tyrosine kinases are enzymes responsible for so-called cascade activation of many proteins through signal transduction. Protease and kinase enzymes enhance the metabolism of foreign substances so kinase inhibition is necessary for the drugs to avoid metabolism and elimination. Proteins are activated by phosphorylation, a step that tyrosine kinase inhibitor inhibit. Almost all the derivatives are having good enzyme inhibitory activity.

As shown in Table 4, the ADME properties are calculated through SwissDock software. Lipophilicity is the ability of a compound to dissolve in the in the lipids, fats, etc. As our body is both made up of both lipid and water, the lipophilicity should be less than >5. If it exceeds, the drug crosses blood-brain barrier and causes central nervous system damage. Water solubility property helps in understanding the solubility of drug in water [31]. As the blood and other body parts are made up of water, it will be easy for the drug to get absorbed and distributed. As shown in Table 3, the compounds are having the capacity to inhibit metabolic enzymes which result in the early metabolism of drug followed by elimination. GLIDE score function is mainly to separate the compounds that bind actively from those that do not, as shown in Table 5. Table 6 shows that the docking results are the binding energies of the ligand compound and target molecule. The higher the binding value, the higher the affinity between ligand and the target molecule which allows the ligand molecule binding to the target molecule and inhibiting or altering its functions or causing cell death, etc. Due to the good binding energies shown by the samples 2, 3, and 4 than the other samples, these samples were further proceed for wet lab synthesis. The synthesized compounds were analyzed through FTIR to identify the molecular structures. The IC_{50} values are estimated through glass prism method. It is the minimum concentration required for *in vitro* assays. The MTT assay is performed for the samples 2, 3, and 4 and the values are shown in Table 9. The MTT assay is used to identify the cell viability in a culture medium. The sample 3 has shown higher value than the other two compounds. Hence, it is further preceded for NR uptake assay. The NR uptake assay is performed and the results showed that the sample 3 has successfully inhibited the cancer cell lines, as shown in Fig. 3.

CONCLUSION

The present study scientifically established the *in silico* design, synthesis, characterization, ADME prediction, and docking studies to predict anticancer activity. We have selected 10 triazole derivatives and all the compounds shown good molecular properties. However, based on the analysis of Lipinski rule of five, only five compounds were passed the rule and so those compounds were further preceded to pharmacokinetic and docking studies. ADME studies have resulted with the three compounds having good solubility, lipophilicity, and enzyme inhibition. From docking scores, we can conclude that these three compounds possess anticancer activity and can be further preceded to wet lab synthesis. The synthesized compounds were identified for their chemical structures through FTIR. The IC_{50} values are determined through glass prism method. The MTT assay and NR uptake assay

were performed and the results showed that the triazole derivative has anticancer activity. These can be further preceded for clinical studies [Fig. 4].

CONFLICTS OF INTEREST

The authors hereby declare that we have no conflicts of interest.

AUTHORS' CONTRIBUTIONS

T. Harshitha – Manuscript preparation. T. Vinay Kumar – Analysis of results and statistical applications. T. Vineetha – Literature review

AUTHORS' FUNDING

Authors have no funding.

REFERENCES

- Bozorov K, Zhao J, Aisaa HA. Triazole-containing hybrids as leads in medicinal chemistry: A recent overview. *Bioorg Med Chem* 2019;27:3511-31.
- Xu Z, Zhao SJ, Liu Y. 1,2,3-Triazole-containing hybrids as potential anticancer agents: Current developments, action mechanisms and structure-activity relationships. *Eur J Med Chem* 2019;183:111700.
- Haider S, Alhusban M, Chaurasiya ND, Tekwani BL. Isoform selectivity of harmine-conjugated 1,2,3-triazoles against human monoamine oxidase. *Future Med Chem* 2018;10:1435-48.
- Scott AT, Weitz M, Breheny PJ, Ear PH, Darbro B, Brown BJ, et al. Gene expression signatures identify novel therapeutics for metastatic pancreatic neuroendocrine tumors. *Clin Cancer Res* 2020;26:2011-21.
- Lewis CS, Thomas HE, Orr-Asman MA, Green LC, Boody RE, Matiash K, et al. mTOR kinase inhibition reduces tissue factor expression and growth of pancreatic neuroendocrine tumors. *J Thromb Haemost* 2019;17:169-82.
- Rawla P, Sunkara T, Gaduputi V. Epidemiology of pancreatic cancer: Global trends, etiology and risk factors. *World J Oncol* 2019;10:10-27.
- Lee JI, Kil JH, Yu GH, Karadeniz F, Oh JH, Seo Y, et al. 3,5-Dicaffeoyl-epi-quinic acid inhibits the PMA-stimulated activation and expression of MMP-9 but not MMP-2 via downregulation of MAPK pathway. *Z Naturforsch C J Biosci* 2020;75:113-20.
- Ugurel S, Röhm J, Ascierio PA, Becker JC, Flaherty KT, Grob JJ, et al. Survival of patients with advanced metastatic melanoma: The impact of MAP kinase pathway inhibition and immune checkpoint inhibition. *Eur J Cancer* 2020;130:126-38.
- Wang X, Xie J, Proud CG. Eukaryotic elongation factor 2 kinase (eEF2K) in cancer. *Cancers (Basel)* 2017;9:162.
- Inokuchi K, Nakayama K, Tauchi T, Takaku T, Yokose N, Yamaguchi H, et al. Therapeutic effects of tyrosine kinase inhibitors and subtypes of BCR-ABL1 transcripts in Japanese chronic myeloid leukemia patients with three-way chromosomal translocations. *Leuk Res* 2018;65:74-9.
- Calderwood SK. HSF1, a versatile factor in tumorigenesis. *Curr Mol Med* 2012;12:1102-7.
- Shomali N, Hatamnezhad LS, Tarzi S, Tamjidifar R, Xu H, Shotorbani SS. Heat shock proteins regulating toll-like receptors and the immune system could be a novel therapeutic target for melanoma. *Curr Mol Med* 2020;13:3432.

13. Gasic I, Groendyke BJ, Nowak RP, Yuan JC, Kalabathula J, Fischer ES, et al. Tubulin resists degradation by cereblon-recruiting PROTACs. *Cells* 2020;9:E1083.
14. Lu Y, Chen J, Xiao M, Li W, Miller DD. An overview of tubulin inhibitors that interact with the colchicine binding site. *Pharm Res* 2012;29:2943-71.
15. Yamamoto KN, Nakamura A, Liu LL, Stein S, Tramontano AC, Inoue Y, et al. Computational modeling of pancreatic cancer patients receiving FOLFIRINOX and gemcitabine-based therapies identifies optimum intervention strategies. *PLoS One* 2019;14:e0215409.
16. Chien ST, Kumar A, Pandey S, Yen CK, Wang SY, Wen ZH, et al. Cancer biology aspects of computational methods and applications in drug discovery. *Curr Pharm Des* 2018;24:3758-66.
17. Hochscherf J, Lindenblatt D, Steinkrüger M, Yoo E, Ulucan Ö, Herzig S, et al. Development of a high-throughput screening-compatible assay to identify inhibitors of the CK2 α /CK2 β interaction. *Anal Biochem* 2015;468:4-14.
18. Popescu T, Lupu AR, Raditoiu V, Purcar V, Teodorescu VS. On the photocatalytic reduction of MTT tetrazolium salt on the surface of TiO₂ nanoparticles: Formazan production kinetics and mechanism. *J Colloid Interface Sci* 2015;457:108-20.
19. Stockert JC, Horobin RW, Colombo LL, Blázquez-Castro A. Tetrazolium salts and formazan products in cell biology: Viability assessment, fluorescence imaging, and labeling perspectives. *Acta Histochem* 2018;120:159-67.
20. Rai Y, Pathak R, Kumari N, Sah DK, Pandey S, Kalra N, et al. Mitochondrial biogenesis and metabolic hyperactivation limits the application of MTT assay in the estimation of radiation induced growth inhibition. *Sci Rep* 2018;8:1531.
21. Stockert JC, Horobin RW, Colombo LL, Blázquez-Castro A. Tetrazolium salts and formazan products in cell biology: Viability assessment, fluorescence imaging, and labeling perspectives. *Acta Histochem* 2018;120:159-67.
22. Chen X, Li H, Tian L, Li Q, Luo J, Zhang Y. Analysis of the physicochemical properties of acaricides based on lipinski's rule of five. *J Comput Biol* 2020;34:2316.
23. Pandey AK, Siddiqui MH, Dutta R. Drug-likeness prediction of designed analogues of isoniazid standard targeting FabI enzyme regulation from *P. falciparum*. 2019;15:364-8.
24. Ishida S. Adme 1Organs-on-a-chip: Current applications and consideration points for *in vitro* ADME-Tox studies. *Drug Metab Pharmacokinet* 2018;33:49-54.
25. Yan G, Wang X, Chen Z, Wu X, Pan J, Huang Y, et al. *In-silico* ADME studies for new drug discovery: From chemical compounds to Chinese herbal medicines. *Curr Drug Metab* 2017;18:535-9.
26. Liu CF, Shen QK, Li JJ. Synthesis and biological evaluation of novel 7-hydroxy-4-phenylchromen-2-one-linked to triazole moieties as potent cytotoxic agents. *Curr Drug Metab* 2017;18:535-9.
27. Farooq S, Hussain A, Qurishi MA, Hamid A, Koul S. Synthesis and biological evaluation of novel 7-hydroxy-4-phenylchromen-2-one-linked to triazole moieties as potent cytotoxic agents. *J Enzyme Inhib Med Chem* 2017;32:1111-9.
28. Madadi NR, Penthala NR. Synthesis and biological evaluation of novel 4,5-disubstituted 2H-1,2,3-triazoles as cis-constrained analogues of combretastatin A-4. *Eur J Med Chem* 2015;103:123-32.
29. Al-Omair MA, Sayed AR, Youssef MM. Synthesis of novel triazoles, tetrazine, thiadiazoles and their biological activities. *Molecules* 2015;20:2591-10.
30. Tim E, Desaulniers JP. Chemical architecture and applications of nucleic acid derivatives containing 1,2,3-triazole functionalities synthesized via click chemistry. *Molecules* 2012;17:12665-703.
31. Onder FC, Durdagi S, Sahin K, Ozpolat B, Ay M. Design, synthesis, and molecular modeling studies of novel coumarin carboxamide derivatives as eEF-2K inhibitors. *J Chem Inf Model* 2020;60:L1766-78.